Cyclopentadienyl and Imide Ligand Transfer from Zirconium to Iridium: Can Early Transition Metal Imido Compounds Be Used as Imide Transfer Reagents?

Patrick L. Holland, Richard A. Andersen,* and Robert G. Bergman*

Department of Chemistry, University of California, Berkeley, California 94720

Received September 19, 1997

Instead of leading to imido group transfer, treatment of $[Cp^*Ir(thf)_3][OTf]_2$ with $Cp_2Zr(N^tBu)(thf)$ ($Cp^* = C_5Me_5$; $Cp = C_5H_5$) gave cyclopentadienyl transfer from Zr to Ir. To characterize the product of this type of reaction more completely, reaction of the corresponding ethyl-substituted compound $[(C_5Me_4Et)Ir(thf)_3][OTf]_2$ with the imidozirconium complex was also carried out. This led to $[Cp^{Et}IrCp][CpZr(NH^tBu)(OTf)_3(thf)]$, which has been crystallographically characterized. An X-ray study of the known pentamethyliridocenium salt $[Cp^*IrCp][BF_4]$ was also performed. In contrast to the above chemistry, the reaction of $Cp^*Ir{-}OCMe_2CMe_2O$ with $Cp_2Zr(N^tBu)(thf)$ gives the heterobinuclear bis(imido) complex $Cp^*Ir(\mu\text{-}N^tBu)_2ZrCp_2$. Thus, in none of these reactions was transfer of the imido group away from the zirconium center observed.

Terminal imido complexes of high-valent and early transition metals are increasingly common, but very few low-valent late transition metal terminal imido complexes have been isolated.[1,2] Presently, the most general route to late transition metal terminal imido compounds is the addition of 2 equiv of a lithium amide to a metal dichloride. This method has been demonstrated by our group for d^6 $Cp^*Ir(NR)$[3] ($Cp^* = C_5Me_5$) and $ArOs(NR)$[4] (Ar = *p*-cymene, C_6Me_6) complexes and has recently been extended to ArRu(NR) complexes by Burrell and co-workers.[5]

This synthetic strategy has two major disadvantages: (a) 1 equiv of amine is released as a byproduct, and this can cause purification problems in the case of nonvolatile arylamines, and (b) the lithium amide is a good reducing agent, which has rendered other imido complexes of the late transition metals inaccessible.[6] We hoped that $Cp_2Zr(NR)(thf)$, which has been studied extensively in these laboratories,[7] would be a milder, more general imide transfer reagent. As a first step in this chemistry, we synthesized various Cp^*IrX_2 complexes with electronegative X ligands (OTf, OR, Cl) and treated these complexes with $Cp_2Zr(N^tBu)(thf)$, hoping to observe ligand transfer to form the known Cp^*IrN^tBu[3] and a Cp_2ZrX_2 byproduct.[8] Although this strategy was unsuccessful in transferring the imido ligand to iridium, these investigations have resulted in two unusual ligand transfer reactions that are described below.

Results and Discussion

When a thf solution of $[Cp^*Ir(thf)_3][OTf]_2$[9,10] was treated with $Cp_2Zr(N^tBu)(thf)$,[7] there was an immediate color change from yellow to a paler yellow. Analysis of the products by ^1H NMR spectroscopy always showed singlets at δ 5.74 and 2.26 ppm, corresponding to the formation of the [Cp*IrCp] cation, but the resonances due to the Zr-containing products were variable.[11] It was possible, however, to extract the iridocenium cation from these reaction mixtures by salt metathesis and aqueous extraction to give pure $[Cp^*IrCp][BF_4]$ (29% yield) or $[Cp^*IrCp][BPh_4]$ (56% yield).

In order to gain insight into the nature of the products, we performed the analogous reaction of $[Cp^{Et}Ir(thf)_3][OTf]_2$ ($Cp^{Et} = C_5Me_4Et$) with $Cp_2Zr(N^tBu)(thf)$; it was possible to grow a single crystal of a product from this reaction. Figure 1 shows an ORTEP diagram of the ion-pair product, $[Cp^{Et}IrCp][CpZr(NH^tBu)(OTf)_3(thf)]$, which crystallized as a diethyl ether solvate. It was possible to refine the structure adequately despite a static disorder of the diethyl ether molecules, which

(1) Wigley, D. E. *Prog. Inorg. Chem.* **1994**, *42*, 239−482.
(2) Cundari, T. R. *J. Am. Chem. Soc.* **1992**, *114*, 7879−7888.
(3) Glueck, D. S.; Wu, J.; Hollander, F. J.; Bergman, R. G. *J. Am. Chem. Soc.* **1991**, *113*, 2041−2054.
(4) Michelman, R. I.; Bergman, R. G.; Andersen, R. A. *Organometallics* **1993**, *12*, 2741−2751.
(5) Burrell, A. K.; Steedman, A. J. *Organometallics* **1997**, *16*, 1203−1208.
(6) Attempts to make the Co and Rh analogues of the Ir imido complex have resulted in an apparent reduction of the metal, and no products could be isolated. Glueck, D. S.; Holland, P. L. Unpublished observations.
(7) Walsh, P. J.; Hollander, F. J.; Bergman, R. G. *Organometallics* **1993**, *12*, 3705−3723.
(8) This type of reaction has been successful for group transfers to main-group elements, see: (a) Fagan, P. J.; Nugent, W. A. *J. Am. Chem. Soc.* **1988**, *110*, 2310−2312. (b) Fagan, P. J.; Burns, E. G.; Calabrese, J. C. *J. Am. Chem. Soc.* **1988**, *110*, 2979−2981. (c) Dufour, P.; Dartiguenave, M.; Dartiguenave, Y. D.; Dubac, J. *J. Organomet. Chem.* **1990**, *384*, 61−69. (d) Breen, T. L.; Stephan, D. W. *Organometallics* **1997**, *16*, 365−369.
(9) White, C.; Thompson, S. J.; Maitlis, P. M. *J. Chem. Soc., Dalton Trans.* **1977**, 1654−1661.
(10) Maitlis, P. M. *Acc. Chem. Res.* **1978**, *11*, 301−307.
(11) We have been unable to reproducibly form a single product from this reaction. We believe that the product variation is due to the amount of trace water and/or excess silver reagent; silylation of the Celite and glassware still gave quantitative Cp transfer but did not give cleaner Zr-containing products.

S0276-7333(97)00827-3 CCC: $15.00
Publication on Web 01/17/1998

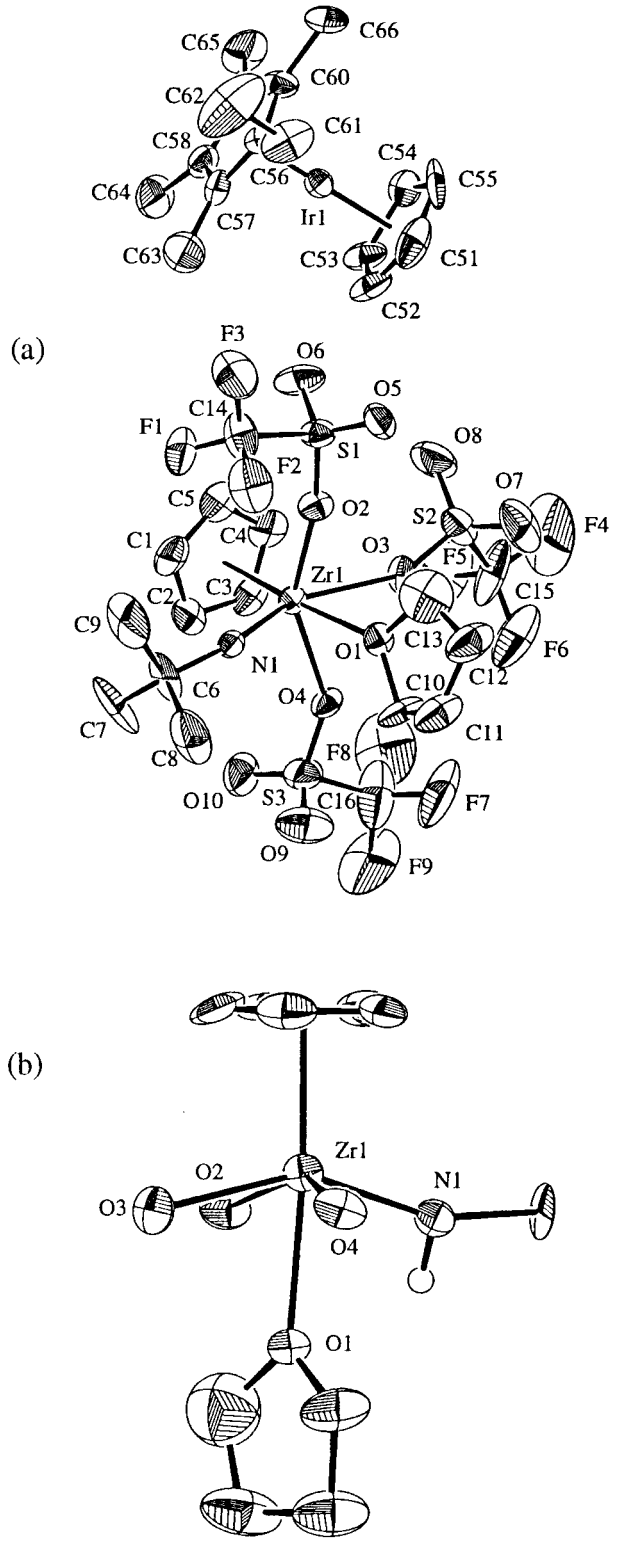

Figure 1. (a) ORTEP diagram of $[Cp^{Et}IrCp][CpZr(NH^tBu)(OTf)_3(thf)]\cdot{}^1/_2Et_2O$, using 50% probability ellipsoids. The diethyl ether solvate is not shown. (b) ORTEP diagram of the $[CpZr(NH^tBu)(OTf)_3(thf)]$ anion. For clarity, only the oxygen atom of each triflate ligand is shown and only the quaternary carbon of the *tert*-butyl group is shown.

lie in columnar channels along the *a* axis of the crystal lattice, well-separated from the rest of the atoms. An ORTEP diagram of the asymmetric unit is shown as Figure 1a; important bond distances and angles are given in Table 1. The iridocenium cation has a planar sandwich structure, as expected for an 18-electron metallocene: the cyclopentadienyl ligands are parallel (dihedral angle = 3.2°), and the Cp(centroid)−Ir−Cp(centroid) angle is 179.1°. The anionic zirconium-containing fragment (Figure 1b) has a four-legged pianostool structure, with Cp(centroid)−Zr−X angles of 102−108°, capped by a tetrahydrofuran ligand trans to Cp. The Zr−O(thf) distance is quite long, 2.379(8) Å; this is similar to the distance of 2.393(3) Å between Zr and the thf ligand trans to Cp in the closely related neutral complex $CpZrCl_3(thf)_2$.[12] The amido NH proton was located in a Fourier map, revealing a trigonal planar geometry at N: this geometry is indicative of the expected π bonding between N and Zr.

Table 1. Important Distances and Angles in $[Cp^{Et}IrCp][CpZr(NH^tBu)(OTf)_3(thf)]\cdot{}^1/_2Et_2O$

	Distances (Å)		
Ir−Cp (centroid)	1.82	Zr−O(1)	2.379(8)
Ir−C(Cp) (ave)	2.18(1)	Zr−O(2)	2.172(8)
$Ir-Cp^{Et}$ (centroid)	1.80	Zr−O(3)	2.254(9)
$Ir-C(Cp^{Et})$ (ave)	2.16(1)	Zr−O(4)	2.194(8)
Zr−Cp	2.22	Zr−N	2.01(1)
Zr−C(Cp) (ave)	2.52(1)		
	Angles (deg)		
$Cp-Ir-Cp^{Et}$	179.1	Cp−Zr−O(3)	102.9
Cp−Zr−O(1)	175.2	Cp−Zr−O(4)	102.5
Cp−Zr−O(2)	103.4	Cp−Zr−N	107.9
O(1)−Zr−O(2)	75.6(3)	O(2)−Zr−N	93.4(4)
O(1)−Zr−O(3)	72.4(3)	O(3)−Zr−O(4)	77.5(3)
O(1)−Zr−O(4)	77.2(3)	O(3)−Zr−N	149.2(4)
O(1)−Zr−N	76.9(3)	O(4)−Zr−N	93.8(4)
O(2)−Zr−O(3)	81.1(3)	Zr−N−C(6)	157.5(9)
O(2)−Zr−O(4)	149.4(3)	twist[a]	8

[a] See text for definition.

Why did the cyclopentadienyl ligand transfer? In terms of hard−soft acid−base theory, the most thermodynamically stable situation results when hard ligands bind to the early transition metal and soft ligands bind to the late transition metal: this is exactly what has happened.[13] The iridium atom has attracted as many soft ligands as possible, leaving the hard oxygen-containing ligands for the zirconium atom. $[Cp^*Ir(solvent)_3]^{2+}$ complexes are known to coordinate various arenes[9] and the cyclopentadienyl ligands of ferrocenes and ruthenocenes,[14] and exchange of cyclopentadienyl ligands at zirconium has been observed,[15,16] indicating that low-barrier pathways for Cp ligand exchange are accessible.

At the time this work was performed, we were surprised to discover that no crystal structure of any iridocene had been reported in the literature.[17] Because of the disorder in the structure described above, we

(12) Erker, G.; Sarter, C.; Albrecht, M.; Dehnicke, S.; Krüger, C.; Raabe, E.; Schlund, R.; Benn, R.; Rufinska, A.; Mynott, R. *J. Organomet. Chem.* **1990**, *382*, 89−102.

(13) The reactions of $[Cp^*Rh(thf)_3]^{2+}$ and $[Cp^*Co(thf)_3]^{2+}$ gave analogous metallocene products, as judged by ^1H NMR spectroscopy.

(14) Herberich, G. E.; Englert, U.; Marken, F.; Hofmann, P. *Organometallics* **1993**, *12*, 4039−4045. In some cases, Cp transfer was observed.

(15) Kondakov, D.; Negishi, E. *Chem. Commun.* **1996**, 963−964.

(16) Peng, M. H.; Brubaker, C. H. *J. Organomet. Chem.* **1977**, *135*, 333−337.

(17) Very recently, a crystal structure of $[Cp^*_2Ir]^+[BPh_4]^-$ has been reported, see: Struchkov, Y. T.; Antipin, M. Y.; Lyssenko, K. A.; Gusev, O. V.; Peganova, T. A.; Ustynyuk, N. A. *J. Organomet. Chem.* **1997**, *536−537*, 281−284. They found a twist angle of 24° and attributed the deviation from an eclipsed geometry to cation−anion steric interactions.

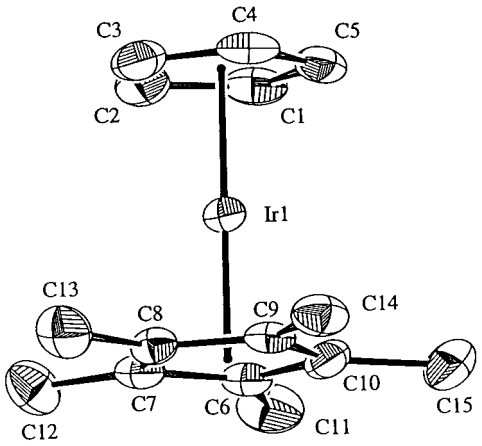

Figure 2. ORTEP diagram of one of the iridocene cations in [Cp*IrCp][BF_4], using 50% probability ellipsoids.

Table 2. Important Distances and Angles in [Cp*IrCp][BF_4]

	distance to centroid (Å)	average Ir−C distance (Å)
Ir(1)−Cp	1.82	2.187(5)
Ir(1)−Cp*	1.80	2.173(5)
Ir(2)−Cp	1.82	2.185(6)
Ir(2)−Cp*	1.80	2.172(5)
		angles (deg)
Cp−Ir(1)−Cp*		179.9
Cp−Ir(2)−Cp*		179.3
twist[a] (molecule 1)		9
twist[a] (molecule 2)		5

[a] See text for definition.

decided to determine the structure of an iridocenium salt with a more conventional anion. Therefore, a crystal of [Cp*IrCp][BF_4][18] was subjected to X-ray crystallographic analysis; an ORTEP diagram showing the two independent molecules in the asymmetric unit is shown in Figure 2, and important bond distances and angles are give in Table 2. As above, the Cp(centroid)−Ir−Cp(centroid) angles are virtually linear (179.9°, 179.3°). Interestingly, in all three independent iridocenium groups (from both crystal structures), the alkylated Cp ring is 0.02−0.03 Å closer to Ir than the unsubstituted Cp ring; the reader is referred to a recent paper for a more complete evaluation of this phenomenon.[14] The twist angle, which describes whether the rings are eclipsed (0°) or staggered (36°), is found to be 5−9° for all three iridocenium groups, showing for the first time the preference for the eclipsed conformation in iridium metallocenes.[17]

In another attempt to effect imido group transfer to the Cp*Ir fragment, the pinacolate complex Cp*$\overline{\text{Ir}-\text{OCMe}_2\text{CMe}_2\text{O}}$[19] was treated with 1 equiv of Cp_2Zr(N-^{t}Bu)(thf) in benzene-d_6, giving 50% conversion to one clean product (by ^{1}H NMR spectroscopy). Addition of a second equivalent of the zirconium imido complex gave ^{1}H NMR spectra indicative of a virtually quantitative yield of this product, which has been identified as Cp*Ir-

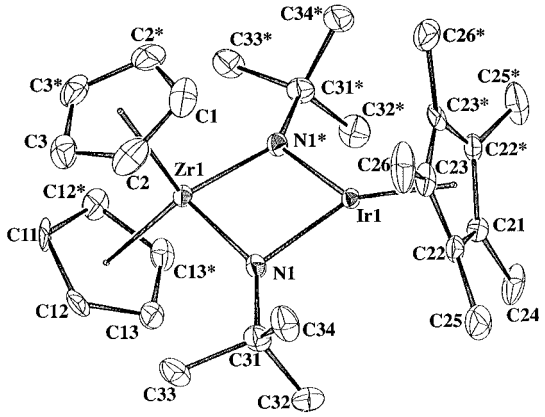

Figure 3. ORTEP diagram of Cp*Ir(μ-N^{t}Bu)$_2$ZrCp_2, using 50% probability ellipsoids.

Table 3. Important Distances and Angles in Cp*Ir(μ-N^{t}Bu)$_2$ZrCp_2

	Distances (Å)		
Ir−Zr	2.9160(6)	Zr-Cp(2)	2.35
Ir−Cp*	1.87	Ir−N	2.046(4)
Zr−Cp(1)	2.37	Zr−N	2.008(4)
	Angles (deg)		
N−Ir−N′	85.6(2)	Ir−N−Zr	92.0(2)
N−Zr−N′	87.6(2)		
Zr−Ir−Cp*	167.0	N−Zr−Cp(1)	110.3
N−Ir−Cp*	137.0	N−Zr−Cp(2)	112.2
Ir−Zr−Cp(1)	109.8	Cp(1)−Zr−Cp(2)	119.7
Ir−Zr−Cp(2)	130.5		

(μ-N^{t}Bu)$_2$ZrCp_2 by X-ray crystallography, as shown in Figure 3 and Table 3. Although our group has crystallographically characterized the very similar complex Cp*Ir(μ-N^{t}Bu)(μ-NPh)ZrCp_2,[20] the previous structure had disorder problems, and so the extremely well-behaved structure (R = 1.6%) here allows better structural characterization of this type of heterobimetallic compound. The four-membered Ir−Zr−N_2 ring is puckered (fold angle = 17.6°), and the nitrogen atoms are planar, indicating π-donation to the formally electronically unsaturated Ir and Zr centers. The Zr−Ir distance is 0.3 Å longer than Zr−Ir single bonds[21] and roughly the same distance as in the several known Cp*Ir(μ-N-^{t}Bu)(μ-X)ZrCp_2 complexes,[20−22] indicating that there is little direct Zr−Ir interaction, as expected for Zr(IV)−Ir(III) complexes. Thus, the puckering is probably steric in origin, as we have observed in other cases where ^{t}Bu groups were present in a hindered four-membered ring.[23]

Clearly, one Zr atom has completely transferred its imido group, leaving $[\overline{Cp_2Zr-OCMe_2CMe_2O}]_n$; we observe a white powder that presumably contains this product. Two mechanistic possibilities for the formation of the bis(imido) complex are shown in Scheme 1. In path A, the desired transfer reaction takes place, giving Cp*IrN^{t}Bu and $\overline{Cp_2Zr-OCMe_2CMe_2O}$. The iridium

(18) Although we used a different synthetic method, pentamethyliridocenium salts have been isolated before, see: Moseley, K.; Kang, J. W.; Maitlis, P. M. *J. Chem. Soc. A* **1970**, 2875−2883.

(19) Glueck, D. S. Unpublished work. The study of this compound and its reactivity are being pursued in our laboratories and will be published in due course. Holland, A. W.; Glueck, D. S.; McCallum, J. S.; Bergman, R. G. Work in progress.

(20) Hanna, T. A.; Baranger, A. M.; Bergman, R. G. *Angew. Chem., Int. Ed. Engl.* **1996**, *35*, 653−655.

(21) Baranger, A. M.; Bergman, R. G. *J. Am. Chem. Soc.* **1994**, *116*, 3822−3835.

(22) (a) Baranger, A. M.; Hanna, T. A.; Bergman, R. G. *J. Am. Chem. Soc.* **1995**, *117*, 10041−10046. (b) Hanna, T. A.; Baranger, A. M.; Bergman, R. G. *Ibid.*, 11363−11364.

(23) Holland, P. L.; Andersen, R. A.; Bergman, R. G. *J. Am. Chem. Soc.* **1996**, *118*, 1092−1104.

Scheme 1

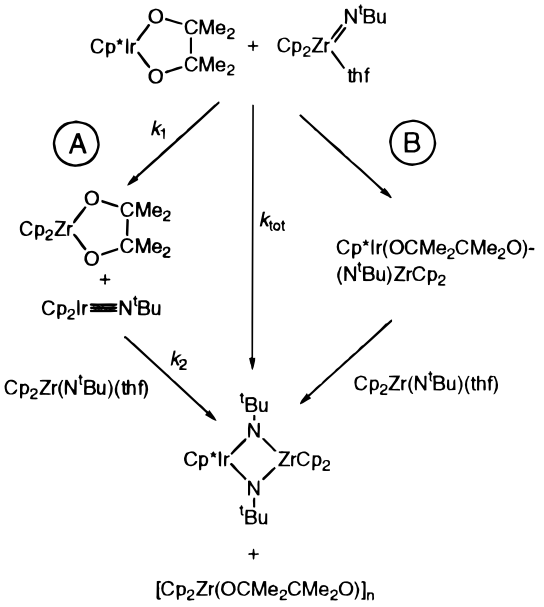

imido complex subsequently reacts with another equivalent of $Cp_2Zr(N^tBu)(thf)$ to generate the observed heterobimetallic species. Consistent with this mechanism, a genuine sample of Cp^*IrN^tBu reacted with $Cp_2Zr(N^tBu)(thf)$ in C_6D_6 to give $Cp^*Ir(\mu\text{-}N^tBu)_2ZrCp_2$. However, the latter reaction proceeded on roughly the *same* time scale as the reaction of $Cp^*\overline{Ir-OCMe_2CMe_2O}$ and $Cp_2Zr(N^tBu)(thf)$ to give this product. If pathway A was being followed and $k_{tot} \approx k_2$, one would expect an observable concentration of the intermediate Cp^*IrN^tBu to build up; however, no intermediates were detected by ^1H NMR spectroscopy. Therefore, the more likely mechanism is path B, in which rate-determining formation of an imido−pinacolate heterobimetallic intermediate is followed by rapid trapping by another Zr imido complex to give the observed product.

Experimental Section

The general procedures used in these laboratories have been described previously.[23] $[Cp^*IrCl_2]_2$ (and $[Cp^{Et}IrCl_2]_2$),[24] $Cp_2Zr(N^tBu)(thf)$,[7] and Cp^*IrN^tBu[3] were prepared by published procedures. Silver trifluoromethanesulfonate (triflate), $NaBF_4$, and $NaBPh_4$ were purchased from Aldrich and used as received. General crystallographic protocols for operating the SMART CCD/area detector system, using SAINT for data reduction and TeXsan for refinement, have been described previously.[23,25]

Typical Synthesis of [Cp*IrCp][ZrL$_n$]. In the glovebox, THF (2 mL) was added to $[Cp^*IrCl_2]_2$ (13.5 mg, 17 μmol) and AgOTf (18.5 mg, 72 μmol). After 5 min of stirring, this mixture turned yellow. It was filtered through Celite (1 cm), and a solution of $Cp_2Zr(N^tBu)(thf)$ (13.5 mg, 37 μmol) in THF (1 mL) was added, causing an immediate color change from yellow to a paler yellow. (If excess AgOTf had been used, a brown precipitate was formed at this stage.) This solution could be reduced to a solid *in vacuo*, or the anion could be exchanged as described below. When the reaction was monitored *in situ* by ^1H NMR spectroscopy (THF-d_8), the following resonances were observed: δ 7.5−6.5 (variable number of Cp singlets), 5.74 (s, 5, Cp), 2.26 (s, 15, Cp*), 1.4−1.0 (variable number of alkyl singlets).

Synthesis of [Cp*IrCp][BF$_4$] and [Cp*IrCp][BPh$_4$] from [Cp*IrCp][ZrL$_n$]. A solution of [Cp*IrCp][ZrL$_n$] in 3 mL of THF (synthesized as described above, using 31 mg of $[Cp^*IrCl_2]_2$, 41 mg of AgOTf, and 30 mg of $Cp_2Zr(N^tBu)(thf)$) was treated with $NaBF_4$ (14 mg, 0.128 mmol), causing no visible change. This was removed from the glovebox, and water (1 mL) was added, causing an immediate loss of color. After addition of additional water (5 mL), the solution was stirred for several minutes and then extracted with CH_2Cl_2 (5 mL) in the air. The CH_2Cl_2 extract was washed with 5 mL of brine and 5 mL of $NaHCO_3$ and dried over Na_2SO_4, and the solvent was evaporated to give $[Cp^*IrCp][BF_4]$ as a white solid that was spectroscopically identical to a sample of $[Cp^*IrCp][BF_4]$ prepared as described below. Yield: 11 mg (29%). An analogous procedure using 16 mg of $[Cp^*IrCl_2]_2$, 21 mg of AgOTf, 15 mg of $Cp_2Zr(N^tBu)(thf)$, and 14 mg of $NaBPh_4$ gave $[Cp^*IrCp][BPh_4]$ as a white solid that was spectroscopically identical to a sample prepared as described below. Yield: 16 mg (56%).

Synthesis of [Cp*IrCp][BF$_4$] from [Cp*IrCl$_2$]$_2$ and NaCp. In the glovebox, a mixture of $[Cp^*IrCl_2]_2$ (316 mg, 0.397 mmol) and NaCp·THF (144 mg, 0.899 mmol) in THF (8 mL) was stirred for 1 day at room temperature. The yellow mixture was treated with $NaBF_4$ (302 mg, 2.75 mmol) and stirred for an additional day. The volatile materials were removed *in vacuo*, and the yellow residue was extracted with CH_2Cl_2 (10 mL), filtered, and concentrated to 3 mL. This orange solution was layered with 3 mL of benzene and allowed to stand at room temperature for 2 days, giving very pale yellow needles of $[Cp^*IrCp]^+[BF_4]^-$ (0.22 g, 58% yield). ^1H NMR (CD_2Cl_2): δ 5.53 (s, 5, Cp), 2.23 (s, 15, Cp*). $^{13}C\{^1H\}$ NMR (CD_2Cl_2): δ 95.3 (C_5Me_5), 81.2 (Cp), 10.7 (C_5Me_5). IR (KBr pellet): 3079 (s), 3038 (s), 2983 (m), 2921 (w), 2850 (w), 1606 (w), 1472 (s), 1455 (m), 1405 (s), 1385 (s), 1300 (w), 1050 (br s), 879 (m), 532 (w), 521 (w). Anal. Calcd for $[Cp^*IrCp][BF_4]$: C, 37.59; H, 4.21. Found: C, 37.86; H, 4.09.

Synthesis of [Cp*IrCp][BPh$_4$] from [Cp*IrCl$_2$]$_2$ and NaCp. This was prepared in an analogous fashion to the BF_4^- salt, using 219 mg of $[Cp^*IrCl_2]_2$, 103 mg of NaCp·THF, and 193 mg of $NaBPh_4$. The product did not crystallize well from CH_2Cl_2/benzene, so it was recrystallized by cooling an acetone solution to −80 °C. Yield: 224 mg (57%). ^1H NMR (CD_2Cl_2): δ 7.37 (m, 2, Ph), 7.06 (t, 2, J = 7.4 Hz, Ph), 6.92 (t, 1, J = 7.2 Hz, Ph), 5.14 (s, 5, Cp), 2.13 (s, 15, Cp*). $^{13}C\{^1H\}$ NMR (CD_2Cl_2): δ 164.5 (q, J_{BC} = 49 Hz, *ipso* Ph), 136.5 (q, J_{BC} = 1 Hz, *meta* Ph), 126.2 (q, J_{BC} = 3 Hz, *meta* Ph), 122.3 (*para* Ph), 95.3 (C_5Me_5), 80.9 (Cp), 11.0 (C_5Me_5). IR (KBr pellet): 3108 (m), 3051 (s), 2982 (s), 2918 (w), 1579 (m), 1478 (s), 1453 (m), 1425 (m), 1408 (m), 1387 (m), 1265 (w), 1139 (w), 1034 (m), 999 (w), 855 (m), 737 (s), 707 (s), 611 (s). Anal. Calcd for $[Cp^*IrCp][BPh_4]$: C, 65.81; H, 5.66. Found: C, 65.38; H, 5.65.

Synthesis of Cp*Ir(μ-N^{t}Bu)$_2$ZrCp$_2$. A solution of $Cp^*\overline{Ir-OCMe_2CMe_2O}$ (45 mg, 0.10 mmol) and $Cp_2Zr(N^tBu)(thf)$ (76 mg, 0.21 mmol) in benzene (5 mL) was heated to 45 °C for 20 h. Over this time, the color changed from red to olive green. The volatile materials were removed *in vacuo*, and the residue was extracted with THF (15 mL). Filtration to remove the white solid gave a green solution that was dried *in vacuo*, to give a spectroscopically pure sample of $Cp^*Ir(\mu\text{-}N^tBu)_2ZrCp_2$ (64 mg, 93% yield). This material could be crystallized by vapor diffusion of pentane into an ether solution to give an analytically pure material and crystals of X-ray quality. ^1H NMR (C_6D_6): δ 5.89 (s, 10, Cp), 1.77 (s, 18, ^{t}Bu), 1.32 (s, 15, Cp*). ^1H NMR (THF-d_8): δ 5.59 (s, 10, Cp), 1.75 (s, 15, Cp*), 1.74 (s, 18, ^{t}Bu). $^{13}C\{^1H\}$ NMR (C_6D_6): δ 108.8 (Cp), 88.8 (C_5Me_5), 67.6 (CMe_3), 36.7 (CMe_3), 12.6 (C_5Me_5). IR (Nujol):

(24) Ball, R. G.; Graham, W. A. G.; Heinekey, D. M.; Hoyano, J. K.; McMaster, A. D.; Mattson, B. M.; Michel, S. T. *Inorg. Chem.* **1990**, *29*, 2023−2025.

(25) Feig, A. L.; Bautista, M. T.; Lippard, S. J. *Inorg. Chem.* **1996**, *35*, 6892−6898.

1445 (sh), 1361 (m), 1346 (s), 1209 (w), 1182 (s), 1066 (w), 1030 (m), 1012 (s), 996 (m), 790 (s), 770 (s), 687 (m). Anal. Calcd for Cp*Ir (μ-N^{t}Bu)$_2$ZrCp$_2$: C, 48.66; H, 6.27; N, 4.05. Found: C, 48.69; H, 6.79; N, 3.92.

Synthesis and X-ray Crystal Structure of [Cp^{Et}IrCp][CpZr(NH^{t}Bu)(OTf)$_3$(thf)]·$^1/_2$Et$_2$O. This compound was synthesized by a method analogous to that for the Cp* analogue above, using 95 mg of [Cp^{Et}IrCl$_2$]$_2$, 179 mg of AgOTf, and 91 mg of Cp$_2$Zr(N^{t}Bu)(thf). The product, after removal of the volatile materials, was extracted into diethyl ether; cooling this solution gave colorless crystals, one of which was used for data collection. ^{1}H NMR analysis showed that the product did not exclusively contain the crystallographically characterized compound.

Inspection of the systematic absences and lattice symmetry indicated space group $P2_12_12_1$; the choice of this space group was confirmed by successful solution and refinement of the structure. A semiempirical ellipsoidal absorption correction (T_{max} = 0.801, T_{min} = 0.507) was applied using SADABS. Of the 18 963 reflections that were measured, 6446 were unique (R_{int} = 4.7%); equivalent reflections were averaged, but Friedel mates were not averaged. The non-hydrogen atoms were refined anisotropically, except for the diethyl ether atoms and C(13), which became nonpositive-definite when refined anisotropically. The positions of the diethyl ether atoms were chosen to give reasonable bond lengths, and they were refined with one-half occupancy, giving reasonable isotropic thermal parameters on these atoms. Hydrogen atoms were included in calculated positions, using fixed isotropic thermal parameters of approximately 1.2 times that of the atom to which they were attached, except for the diethyl ether molecule, which was modeled without hydrogens. The final cycle of full-matrix least-squares refinement was based on 5043 observed reflections ($I > 3\sigma(I)$) and 529 variable parameters and converged with unweighted and weighted agreement factors of R = 4.62%, R_w = 5.14%, and GOF = 1.55. Using all unique data: R = 6.10%, R_w = 5.45%.

X-ray Crystal Structure of [Cp*IrCp][BF$_4$]. Recrystallization of [Cp*IrCp][BF$_4$] by slow evaporation of acetone gave clear blocks. The systematic absences uniquely indicated space group $P2_1/c$. A semiempirical ellipsoidal absorption correction (T_{max} = 0.986, T_{min} = 0.723) was applied. Of the 15 338 reflections that were measured, 5876 were unique (R_{int} = 2.7%); equivalent reflections were averaged. The non-hydrogen atoms were refined anisotropically, and hydrogen atoms were placed in calculated position with fixed isotropic thermal parameters of approximately 1.2 times that of the atom to which they were attached. During the final stages of refinement, a model was used in which three fluorine atoms of one BF$_4$ group were rotationally disordered; these atoms were included with one-half occupancy. Anisotropic refinement of these atoms converged with reasonable anisotropic thermal motion. The final cycle of full-matrix least-squares refinement was based on 4617 observed reflections ($I > 3\sigma(I)$) and 406 variable parameters and converged with unweighted and weighted agreement factors of R = 2.24%, R_w = 2.85%, and GOF = 1.28. Using all unique data: R = 3.18%, R_w = 3.13%.

X-ray Crystal Structure of Cp*Ir(μ-N^{t}Bu)$_2$ZrCp$_2$. The systematic absences and lattice symmetry did not distinguish between several possible space groups; the choice of *Abm*2 was confirmed by successful solution and refinement of the structure. A semiempirical ellipsoidal absorption correction (T_{max} = 0.862, T_{min} = 0.752) was applied using SADABS. Of the 5472 reflections that were measured, 1979 were unique (R_{int} = 2.7%); equivalent reflections were averaged. The molecule lies on a mirror plane which passes through Ir, Zr, C(1), C(11), C(21), and C(24); the symmetry-related atoms within the molecule are related by the operation (x, $^1/_2 - y$, z). In initial refinement, the non-hydrogen atoms were refined isotropically; at this stage, the correct enantiomorph was determined by comparing the R values for the correct structure (R = 2.6%) to the inverted structure (R = 6.6%). The non-hydrogen atoms were refined anisotropically, and hydrogen atoms were located and their positions were refined using fixed isotropic thermal parameters of approximately 1.2 times that of the atom to which they were attached. The final cycle of full-matrix least-squares refinement was based on 1864 observed reflections ($I > 3\sigma(I)$) and 217 variable parameters and converged with unweighted and weighted agreement factors of R = 1.61%, R_w = 2.00%, and GOF = 0.77. Using all unique data: R = 1.64%, R_w = 2.02%.

Acknowledgment. The authors thank the National Institutes of Health (Grant No. GM-25459) for funding and Dr. F. J. Hollander for help in determining the crystal structures, especially that of Cp*Ir(μ-N^{t}Bu)$_2$ZrCp$_2$.

Supporting Information Available: Tables of data collection parameters, metrical data, positional parameters, and anisotropic thermal parameters for the crystal structures and an ORTEP diagram of the entire asymmetric unit of [Cp*IrCp][BF$_4$] (21 pages). Ordering information is given on any current masthead page.

OM970827A